

CERN LIBRARIES, GENEVA



CM-P00048659

CERN/ISRC/74-38
27 August 1974*)

A PROPOSAL
TO EXTEND THE OBJECTIVES OF THE EXPERIMENT R604
TO A SEARCH OF ELECTRONS AND MUONS
DIRECTLY PRODUCED IN THE FORWARD DIRECTION:
A HUNT FOR CHARMED PARTICLES

L. Baum	A. Kernan	A. Orkin-Lecourtois
M. Block	V. Kukhtin	C. Rubbia
J. Crawford	J. Layter	D. Schinzel
A. Derevshchikov	W. Marsh	B. Shen
R. Glauber	F. Muller	A. Staude
T. Golutvin	P. McIntyre	G. Tarnopolsky
H. Hilscher	B. Naroska	V. Telegdi
J. Irion	M. Nussbaum	R. Voss

CERN, Geneva, Switzerland

Department of Physics, Harvard University,
Cambridge, Mass., USA.

Sektion Physik der Universität, Munich, Germany

Northwestern University, Evanston, Ill., USA

University of California in Riverside,
Riverside, Calif., USA

(R604 Collaboration)

*) Happy 49th birthday F Muller

ABSTRACT

We propose to add to the R604 set-up an electron telescope and a hadron absorber to identify muons by penetration in order to perform a sensitive search for charmed particles produced in the forward-direction. The signature for the events is the simultaneous production of a muon and an electron, possibly associated with an anomalously copious strange particle production (Λ^0 and K^0). The set-up would also permit us to extend the study of the inclusive direct electron production and the di-muon production to angles less than 15° . If vector mesons are responsible for the observation of di-leptons, their production and hadronic decay will be observed with good efficiency by the R604 set-up.

1. PHYSICS OBJECTIVES

Three independent groups at NAL^{1,2,3)} have observed an inclusive, direct muon production around 90° in the centre-of-mass in proton-proton collisions at high energies. This confirms the earlier observation of the effect at Serpukhov⁴⁾ A corresponding direct production of electrons has been reported at NAL³⁾ and at the ISR⁵⁾.

The phenomenon appears as an anomaly and it cannot be explained easily Briefly, inclusive particle production at 90° is characterized by the variables p_T and $s = 2mE_p$ Data exist for $1 \text{ GeV} < p_T < 7 \text{ GeV}$ and $60 \text{ GeV} < E_p < 300 \text{ GeV}$ Although the μ yield varies by several orders of magnitude over the range of kinematic variables, the μ/π ratio remains approximately constant. Furthermore, the ratio μ/π has a surprisingly large value of 10^{-4} Neither the yield nor the kinematical independence of the effect have been satisfactorily explained in terms of the simple quark-antiquark annihilation model, which predicts typically yields 10^{-2} to 10^{-3} of what is observed. (Incidentally, we remark that the model gives on the contrary an excellent account of the di-muons observed at BNL by Lederman et al. for $E_p = 29 \text{ GeV}$). Alternatively, if we assume a vector meson production and a subsequent decay into muon pairs we would require for the ϕ , which has the largest branching ratio into muon pairs, a ϕ production cross-section (at 90°) several times greater than the one for pions Although not excluded by experiment, this alternative is rather unlikely

Obviously we need some novel mechanism for enhancement of the muon and electron yields at high energies. A fashionable alternative is the production of pairs of particles C and \bar{C} , which possess some novel quantum number ("charm") forbidding both strong and electromagnetic decays of C and \bar{C} into ordinary^{*)} particles. Eventually, $C(\bar{C}) \rightarrow \mu^\pm + \nu_\mu + \text{ordinary particles}$, or $C(\bar{C}) \rightarrow e + \nu_e + \text{ordinary particles}$,

*) The term "ordinary" as used here includes strange particles. In fact, according to present views, the leptonic decays of charmed particles lead preferentially to strange hadrons.

via weak interactions. Well above threshold, the C-production could obey strong interaction scaling, which would explain the approximate constancy of the μ/π ratio. The decay branching ratios into muon and electrons are equal, thus explaining the approximate equality of the muon and electron yields.

Whatever the true mechanism might finally turn out to be, the phenomenon is an important one and requires extensive experimental investigation. Several fundamental questions are as yet unanswered; they motivate the present proposal:

- 1) Is the total charged lepton yield an over-all large effect of the order of 10^{-4} of the pions, or is one observing a local enhancement limited to 90° ? The most elementary approach to this question is to measure the lepton and electron yields in the forward directions, where the majority of the pions are emitted.
- 2) What is the nature of the associated lepton(s), i.e. are they always $\mu^-\mu^+$ or e^-e^+ pairs, as one would expect in the case of electromagnetic interactions, or is there an appreciable fraction of cases in which neutrinos and electrons (or muons) are also emitted in the process, as one would expect for the decay of C, \bar{C} pairs? If, for example, $C \rightarrow \mu^+ + \nu_\mu +$ ordinary particles and $\bar{C} \rightarrow e^- + \bar{\nu}_e +$ ordinary particles, then one could observe simultaneous direct production of an electron and a muon of opposite charge. We believe that this would be significant evidence for charmed particles.
- 3) If real di-muons are produced, what is their invariant mass distribution, i.e. is it mainly of a resonant nature (vector mesons) or does one observe instead a continuum?

We propose to perform a number of measurements with the R604 detector with two important additions:

- i) a steel filter between the source (diamond) and the detector to separate out muons by penetration. Only a relatively small absorber is required, since muons traverse it at a small incidence

angle. The absorber must be as close as possible to the source in order to minimize the probability of $\pi \rightarrow \mu$ decays in flight;

- ii) a simple electron telescope consisting of scintillation counters, wire chambers, gas Cerenkov counter, a shower detector, and a total absorption lead-glass counter to identify electrons. The acceptance of the telescope is $\sim 2 \times 10^{-3}$ sterad at a predetermined production angle of about 15° . Dalitz pairs and gamma rays converting in the vacuum chamber window are removed by pulse-height requirements in the first scintillators³⁾

The electron telescope has an excellent rejection capability for hadrons and for electron-positron pairs produced by conversion of photons (either in the material of the detector or by internal conversion (Dalitz pairs)). A careful subtraction of the γ -background can be performed by extrapolation of measurements with thin radiators added to the vacuum window. Hence a meaningful search for direct electron production in the forward angles is one of the first objectives of our experiment. The situation is less favourable for the observation of direct muon production. The main background to this measurement is a $\pi \rightarrow \mu$ decay before hadrons are absorbed by the filter. The background is more severe at the ISR than at NAL because observations are made on slower particles. The determination of the direct yield has to be performed as customary by extrapolation to zero decay path^{1,2)}. The decay path can be varied by moving vertically both beams by several millimetres. A remarkable property of the R604 spectrometer is that, because of its up-down symmetry, the sum of events due to $\pi \rightarrow \mu$ decays with muons going up and down is independent of the displacement, thus providing an accurate internal monitor for the extrapolation. However, the background due to decays in flight is large and the direct production may only be a few per cent of the background. For instance at $p = 7$ GeV, $\theta = 5^\circ$ the apparent μ/π due to decays is $\approx 5 \times 10^{-4}$ with the beam 1 cm away from the vacuum chambers. Evidently this method is not very convincing if the effect at small angles is somewhat smaller than at 90°

For those reasons we would like to concentrate on the determination of the cross-section for di-muon production, as a function of the relevant kinematical quantities, like invariant mass, total momentum and angle, and momentum unbalance of the pair. The decays of the hadrons before absorption are no longer a problem since now one has to generate two muons in a single interaction. The di-muon signal should be backgroundless. A rough estimate of the event rate is ~ 15 ev/sec for $L = 10^{30}$ $\text{cm}^{-2} \text{ s}^{-1}$, $\mu/\pi \sim 10^{-4}$, and an average detection efficiency of 0.2, which is a reasonable estimate for $m_{\mu\mu}$ peaking around 1-2 GeV. A careful, high statistics experiment is clearly possible even if the relative μ/π yield at forward angles is considerably less than the inclusive yield observed around 90° . As mentioned earlier, a very exciting possibility is that an appreciable number of electron-muon pairs are produced, as the result of the weak decays of a pair of particles. If charmed particles are produced, one expects to observe an anomalously copious production of strange particles. For this reason, the angular range $\lesssim 50$ mrad, has not been covered by the iron shield, and it will be used to detect Λ^0 and K^0 decays. The aperture offers also a reasonable acceptance for hadronic decays of vector mesons and it can be used to calibrate the spectrometer with scattered protons.

2. THE EXPERIMENTAL SET-UP

The experimental set-up is shown in Figs. 1 2a and 2b. The apparatus can be sub-divided into three items:

- i) Magnetic spectrometer and muon filter in arm 1;
- ii) Electron telescope in arm 1;
- iii) Hadron detector in arm 2, consisting of wire chambers and calorimeter, as in R604 proposal.

2.1 The magnetic spectrometer in arm 1

The magnetic spectrometer in arm 1 equipped with multiwire proportional chambers stays essentially in the configuration described in CERN/ISRC/74-3. In addition, we plan to add a muon filter in front of the spectrometer as shown in Fig. 1. In order to minimize the pion decay path the vacuum chambers of the interaction region and the first 60 cm of arm 1 is made as flat as possible, using standard elliptical pipes.

In addition, at 15° to the arm 1 beam pipe, a thin window is provided to allow electrons to enter the electron spectrometer, which will be described in Section 2.2.

The muon filter is shown in Fig. 2a. It consists of three parts:

- 1) The first part, $50 \times 30 \times 15 \text{ cm}^3$ iron, positioned as close as possible to the beam line, is made easily removable in order to measure the particle rate through the small chambers.
- 2) The second part, which is an iron-scintillator sandwich with dimensions $70 \times 120 \times 25 \text{ cm}^3$, is used to confirm that an outgoing particle does not interact in the iron. This part of the muon filter can also be magnetized in order to increase the acceptance of the spectrometer. The magnetization of this part requires 2000 A-turns and increases the spectrometer acceptance for a 5 GeV muon from 110 mrad to 150 mrad.
- 3) The third part is shaped in order to ensure that any particle emitted at angles greater than 50 mrad will traverse 1.2 m of iron.

The second and third parts of the muon filter and the vacuum pipe are designed to allow possible Λ^0 decay products of less than ~ 50 mrad to enter the spectrometer (cf. Fig 2a).

With a test arrangement, using the R604 calorimeter, we have measured the effective interaction length of 17 GeV π^- in Fe and found it to be ~ 11 cm (Fig. 3) Using the sampling of the hadronic shower both by a series of scintillators and a few "early" MWPC's, as well as by measuring the momentum of the emerging particle, we expect to attain a hadron rejection close to the "theoretical" value $e^{-120/11} \approx 2 \times 10^{-5}$. The muon energy loss is about 1.4 GeV.

In between the first two parts of the filter, the already existing small chambers can measure particles as close as 8 mm from the pipe. Their purpose is to check that a track, reconstructed in the spectrometer, traversed most of the filter without interacting. They will also be used to improve the track reconstruction for accepted muons.

2.2 The electron telescope

We describe the various parts of the e^- telescope in detail:

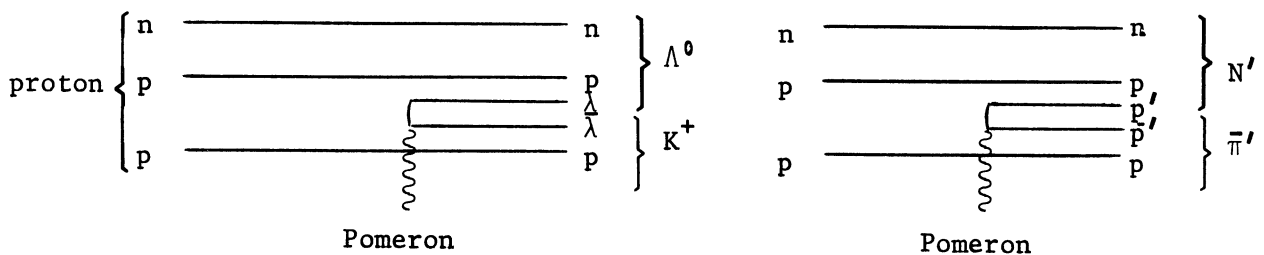
- i) The vacuum chamber window will be roughly $10 \times 5 \text{ cm}^2$, and as thin as possible to minimize pair production and other electromagnetic processes. The effect of the remaining thickness will be checked by inserting additional material in front of the window, and extrapolating to zero thickness.
- ii) The chambers in front of the magnet are MWPC, having $10 \times 10 \text{ cm}^2$ sensitive area, with 10μ wires spaced at 1 mm, as used in R602. The rear chambers are similar with a sensitive area of $40 \times 10 \text{ cm}^2$ with a wire spacing of 1 mm in the momentum defining coordinate, and 2 mm in the other.
- iii) The magnet is a standard MNP08 shimmed out to give a gap of 10 cm. Its gap length is 125 cm and its gap width is 20 cm. In this configuration it should have $\int B \cdot dl \sim 1 \text{ Tm}$, giving 5° bending at 3.5 GeV/c. It can, if necessary, be powered in series with the main spectrometer magnet, using the existing power supply.
- iv) The Cerenkov counter is based on a standard CERN design, with a non-standard 1.45 m long radiator box to fit inside the magnet. With air at atmospheric pressure as a radiator, the pion threshold is 5.6 GeV. With a normal bi-alkali photocathode, a relativistic electron yields a signal of ~ 10 photoelectrons. If a UV sensitive cathode is used, the signal increases to ~ 25 photoelectrons. In addition to its use in the trigger, the output-signal of the Cerenkov counter will be digitized and recorded.
- v) The shower detector consists of three parts, a 2 radiation length lead scintillator sandwich, MWPC's and a 15 rad. length long lead-glass Cerenkov counter. The lead-glass is in the form of three adjacent hexagonal blocks, giving a sensitive area of $\sim 40 \times 12 \text{ cm}^2$. The development of the shower can therefore be followed, allowing an additional check on the nature of the detected particle. The resolution of the lead-glass counter alone has been measured to be 5% ⁶⁾.

3. EFFICIENCY AND RATES FOR THE DETECTION OF CHARMED PARTICLES

In the following, we assume that charmed particles are constructed by adding a fourth quark p' ($Q = 2/3$, $I = 0$, $S = 0$, charm $C = +1$) to the (p, n, λ) quark triplet (see Charm Chart, Table 1). The selection rules $\Delta C = \Delta Q$ and $\Delta S = \Delta Q$ ensure that leptonic decays of charmed particles (antiparticles) always yield positively (negatively) charged leptons. Moreover the decay of non-strange charmed particles produce predominantly strange baryons and mesons. For masses $\gtrsim 3$ GeV their lifetime is very short ($< 10^{-13}$ sec, see Fig. 4) and leptonic decay modes (i.e. $N' \rightarrow \Lambda \ell^+ \nu$, $\pi' \rightarrow \bar{K} \ell^+ \nu$) are expected to dominate over non-leptonic modes (see Fig. 4) In summary, we expect the charmed particle decays to yield mostly both a lepton and a strange particle.

As regards the production mechanism of charmed particles, conservation of charm in strong interactions implies either pair production $\pi' \bar{\pi}'$, $N' \bar{N}'$ or associated charm production $N' \bar{\pi}'$. The first mechanism may be compared to $K\bar{K}$, baryon-antibaryon production, and would be expected to exhibit a rather flat rapidity distribution (as predicted for instance by a multi-peripheral model). In contrast, associated charm production, by analogy with YK , may be expected to take place preferentially for x values closer to 1, as in the Fig. 5 for the inclusive Λ spectrum observed in a bubble chamber at NAL (reported by M. Jacob at 1972 Batavia Conference). Subtracting a flat rapidity background, these data yield a cross-section for forward production processes, presumably diffractive, of about 1/3 of the total Λ production, i.e. about 0.6 mb in each hemisphere. This can be compared to the total diffraction cross-section (~ 4 mb at each vertex), yielding an upper limit of $\sim 15\%$ for Λ decays of excited protons. [We note that the N_{1780}^* has a YK branching ratio between ~ 7 and 14% .]

The diffractive ΛK and $N' \bar{\pi}'$ production processes may be visualized in the quark picture as below



On the basis of the above estimate of the branching ratio for ΛK final states, we shall make the conservative working hypothesis of a branching ratio of 10^{-3} for the decay of excited protons into $N'\bar{\pi}'$. The cross-section for the diffractive process $p_1 p_2 \rightarrow X p_2$ with $M_x^2 \geq 25 \text{ GeV}^2$ being $\sim 0.8 \text{ mb}$ (Akimov et al., NAL Conf. 78/56-EXP), the anticipated cross-section for associated charmed particle production by diffraction would then be $\sim 1 \text{ } \mu\text{b}$. We note that the value of 10^{-3} assumed for the branching ratio corresponds to a $1 \text{ } \mu\text{b}$ cross-section for the reaction Pomeron-proton $\rightarrow N'\bar{\pi}'$ at $s \geq 25 \text{ GeV}^2$ (we use the value of 1 mb for $\sigma_{\mathbb{P}p}$ as given by G.F. Chew, Stony Brook Conference 1973).

We have calculated efficiencies and detection rates under the following assumptions:

- 1) 26 GeV p-p ISR collisions;
- 2) $M_{N'} = 3 \text{ GeV}$, $M_{\bar{\pi}'} = 2 \text{ GeV}$;
- 3) The reaction $p_1 + p_2 \rightarrow (N'\bar{\pi}')^+ p_2$ is used as a model to estimate, via the quark picture, that the average longitudinal momentum of the baryon N' is $\frac{2}{3} \times 26 \approx 17 \text{ GeV}$, whereas the $\bar{\pi}'$ has $\frac{1}{3} \times 26 \approx 9 \text{ GeV}$ momentum, and the opening angle between them is taken as zero;
- 4) Zero degree production of the $(N'\bar{\pi}')^+$ system;
- 5) Isospin conservation and the quark model (see Charm Chart) allow us to determine the relative production rates of $I = 0$ (N'_0) and $I = 1$ (N'_1) charmed baryons:

$$\begin{aligned} p_1 + p_2 \rightarrow (N'_1{}^{++} \bar{\pi}^+) p_2 &: 2 \\ &(N'_1{}^+ \bar{\pi}'^0) p_2 : 1 \\ &(N'_0{}^+ \bar{\pi}'^0) p_2 : 3 \end{aligned}$$

- 6) The weak decay modes are taken to be exclusively 3-body leptonic modes, with equal electron-muon rates, always yielding strange particles, i.e. we assume that

$$\left. \begin{aligned} N'^{++} &\rightarrow \Sigma^+ \ell^+ \nu_\ell \\ \bar{\pi}^+ &\rightarrow K^0 \ell^- \bar{\nu}_\ell \end{aligned} \right\}$$

or

$$\left. \begin{aligned} N'^+ &\rightarrow \Sigma^0 (\Lambda^0) \ell^+ \nu_\ell \\ \overline{\pi'^0} &\rightarrow K^+ \ell^- \overline{\nu}_\ell \end{aligned} \right\}$$

equally divided between $\ell^+ = \mu^+$ and e^+ and $\ell^- = \mu^-$ and e^- .

- 7) Only muons of momenta greater than 2.5 GeV/c and electrons with momenta less than 6 GeV/c are accepted in the spectrometers.

The following table gives the efficiencies for detection of the Λ 's, e^+ , e^- , μ^+ and μ^- , from the above three-body decays, calculated in the conventional way.

Table of Efficiencies for Particle Detection

μ^+	μ^-	e^+	e^-	$\Lambda^0 \rightarrow \pi^- p$
0.17	0.09	3.3×10^{-3}	3.8×10^{-3}	0.01

On the basis of a luminosity corresponding to 10^5 events/sec, for a $\sigma_{\text{tot}} \approx 40$ mb, the following rates are computed:

Rate Table

Event signature	Rate
a) $e^+ \cdot p_2$ or $e^- \cdot p_2$	~ 1 per 4 minutes
b) $(e^+ \cdot \mu^-) \cdot p_2$ $(e^+ \cdot \Lambda^0) \cdot p_2$	~ 1 per 1.5 hours ~ 1 per 10 hours
c) $(e^- \cdot \mu^+) \cdot p_2$ $(e^- \cdot \Lambda^0) \cdot p_2$	~ 1 per 0.7 hours ~ 1 per 9 hours
d) $(\mu^+ \cdot \mu^-) \cdot p_2$	~ 1 per 1.7 minutes

Since we have assumed a diffractive process, there is -- at least for single diffraction -- a fast proton at small angle in Arm 2. We can identify this proton (and eventually use it as an extra trigger requirement) by placing in Arm 2 the small ($10 \times 10 \text{ cm}^2$) wire chambers of experiment R602, possibly followed by the R604 calorimeter for energy definition.

We emphasize that whereas these rates are calculated for a diffractive process of $1 \mu\text{b}$ cross-section, other forward production processes will also be detected in the spectrometer.

Also, as shown in the Charm Table, there exists the possibility of producing higher charm ($C = +2$, and $+3$) baryons diffractively, although the energy thresholds are expected to be higher.

Table 1
Charm Chart

Particle family name	C	S	B	I	I _Z	Q	Quark composition	Favored types of leptonic decay modes
π'	+1	0	0	1/2	+1/2	+1	$p'\bar{n}$	$\pi'^+ \rightarrow \bar{K}^0 \ell^+ \nu$ $\pi'^+ \rightarrow K^- \pi^+ \ell^+ \nu$
					-1/2	0	$p'\bar{p}$	$\pi'^0 \rightarrow K^- \ell^+ \nu$ $\pi'^0 \rightarrow \bar{K}^0 \pi^- \ell^+ \nu$
K'	+1	+1	0	0	0	+1	$p'\bar{\lambda}$	$K'^+ \rightarrow \bar{K}^0 \ell^+ \nu$ $K'^+ \rightarrow K^- \pi^+ \ell^+ \nu$
N'	+1	0	+1	1	+1	+2	$p'pp$	$N_1'^{++} \rightarrow \Sigma^+ \ell^+ \nu$ $N_1'^{++} \rightarrow \Sigma^0 (\Lambda^0) \pi^+ \ell^+ \nu$
					0	+1	$p'pn$	$N_1'^+ \rightarrow \Sigma^0 (\Lambda^0) \ell^+ \nu$ $N_1'^+ \rightarrow \Sigma^\mp \pi^\pm \ell^+ \nu$
					-1	0	$p'nn$	$N_1'^0 \rightarrow \Sigma^- \ell^+ \nu$ $N_1'^0 \rightarrow \Sigma^0 (\Lambda^0) \pi^- \ell^+ \nu$
				0	0	+1	$p'pn$	$N_0'^+ \rightarrow \Sigma^0 (\Lambda^0) \ell^+ \nu$ $N_0'^+ \rightarrow \Sigma^\mp \pi^\pm \ell^+ \nu$
Λ'	+1	-1	+1	1/2	+1/2	1	$p'p\lambda$	$\Lambda'^+ \rightarrow \Xi^0 \ell^+ \nu$ $\Lambda'^+ \rightarrow \Xi^- \pi^+ \ell^+ \nu$
					-1/2	0	$p'n\lambda$	$\Lambda'^0 \rightarrow \Xi^- \ell^+ \nu$ $\Lambda'^0 \rightarrow \Xi^0 \pi^- \ell^+ \nu$
Ξ'	+1	-2	+1	0	0	0	$p'\lambda\lambda$	$\Xi'^0 \rightarrow \Omega^- \ell^+ \nu$

- Rules: 1) $\Delta C = \Delta Q$ for all leptonic decays
 2) $\Delta S = \Delta Q$ for strangeness-changing leptonic decays, $\Delta I = 0$

Possible production mechanism in strong interactions ($\Delta S = 0$, $\Delta Q = 0$, $\Delta B = 0$, $\Delta C = 0$)

- 1) Pair production $\pi'\bar{\pi}'$, $K'\bar{K}'$, $N'\bar{N}'$, $\Lambda'\bar{\Lambda}'$, $\Xi'\bar{\Xi}'$,
- 2) "Associated Charm" production proton $\rightarrow (N'\bar{\pi}')^{+1}$
 neutron $\rightarrow (N'\bar{\pi}')^0$

Note: we cannot have proton $\rightarrow (\Lambda'\bar{K}')^{+1}$ } since $\Delta S \neq 0$ although
 or neutron $\rightarrow (\Lambda'\bar{K}')^0$ } $\Delta C = 0$,

but we can have proton $\rightarrow (\Lambda'\bar{K}'KK)^+$
 and proton $\rightarrow (\Xi'\bar{K}'KKK)^+$, etc.,

- 3) We expect diffractive production of $p \rightarrow N'^{++} \pi'^+$ and $N'^0 \pi'^0$,
 in analogy to $\Lambda K \left\{ \begin{array}{l} \Sigma^+ K \\ \Sigma^0 (\Lambda^0) K \end{array} \right\}^+$

Table 1 (cont'd)
Charm Chart

Particle Family Name	C	S	B	I	I _z	Q	Quark composition	Favored types of leptonic decay modes
N''	+2	0	1	1/2	+1/2	+2	p'p'p	$\left. \begin{aligned} N''^{++} &\rightarrow \Lambda'^+\pi^+(\pi^0) \\ &\rightarrow \Lambda'^0\pi^+\pi^+ \end{aligned} \right\}$ $N''^+ \rightarrow \Lambda'^+\pi^0(\pi^0)$ $\rightarrow \Lambda'^0\pi^+$ <p>and, in a <u>second weak decay</u>, the Λ''s decay into Ξ's and $\ell^+\nu$</p>
					-1/2	+1	p'p'n	
Λ''	+2	-1	1	0	0	+1	p'p' λ	$\Lambda''^+ \rightarrow \Xi'^0\pi^+$ <p>and, in a <u>second decay</u>, $\Xi'^0 \rightarrow \Omega \ell^+\nu$</p>
N'''	+3	0	1	0	0	+2	p'p'p'	$N'''^{++} \rightarrow \Lambda''^+ + \pi^+,$ <p>and, in <u>next decay</u></p> $\Lambda''^+ \rightarrow \Xi'^0\pi^+,$ <p>and in <u>next decay</u></p> $\Xi'^0 \rightarrow \Omega \ell^+\nu$

1) Strong interaction production mechanisms:

- a) Pair production: $N''\bar{N}''$, $\Lambda''\bar{\Lambda}''$, $N'''\bar{N}'''$.
- b) "associated charm" production proton $\rightarrow (N''\bar{\pi}'\bar{\pi}')^+$, $(\Lambda''\bar{K}'\bar{K}'KKK)^+$, $(N'''\bar{\pi}'\bar{\pi}'\bar{\pi}')^+$ + $(N'''\bar{K}'\bar{\pi}'\bar{\pi}'K)^+$, etc.

Note: No C = +2 or +3 (multiple charm) mesons are possible.

Notation: Quark $\left. \begin{array}{l} p' : I = 0 \quad Q = 2/3 \\ p : I = 1/2 \quad Q = 2/3 \\ n : I = 1/2 \quad Q = -1/3 \\ \lambda : I = 0 \quad Q = -1/3 \end{array} \right\}$

I = isospin

Q = charge

S = strangeness

I_z = z-component of I

B = baryon number

C = charm (0, ± 1 , ± 2)

4. DI-MUONS FROM STANDARD PROCESSES

There are four sources:

- 1) π - μ decay of two simultaneously produced π 's;
- 2) one π - μ , one K - μ ;
- 3) $K_{\mu 3}$ with subsequent $\pi \rightarrow \mu$ decay;
- 4) $V \rightarrow 2\mu$ electromagnetic decays.

We have considered only (1) in detail. (2) contributes only a correction to (1), of the order of +10%. (3) is a decay process with a maximum transverse momentum of 0.21 GeV/c. The minimum accepted transverse momentum, using a pessimistic lower cut-off of 2.5 GeV for both muons, is $2 \times 50 \text{ mrad} \times 2.5 \text{ GeV} \approx 0.25 \text{ GeV/c}$.

The electromagnetic decays of vector mesons (ϕ, ρ, ω) will not be discussed here, since they constitute a possible object of investigation rather than a background. In any case, the spectrometer measures the invariant mass of the two μ 's, and thus discriminates effectively.

We have calculated the "effective cross-section" $\sigma_{\mu+\mu^-}$ for detecting two muons from π - μ decays in the following way:

The apparatus has an arbitrary lower cut-off p_{μ}^{min} (say 2.5 GeV/c), and an angular acceptance $50 \text{ mrad} < \theta < 110 \text{ mrad}$. To allow for π - μ decay kinematics, we assumed that pions with $p_{\pi} = p_{\mu}/0.8$ are the effective parents of the muons with momentum p_{μ} .

To integrate the pion production cross-sections as a function of p_{π} and θ , we have transformed the existing data on invariant cross-section as follows

$$\sigma_{\pi} = \int \left(E \frac{d^3\sigma}{dp^3} \right) \frac{dp_{\ell} dp_t^2}{E} \approx 2\pi \int \left(E \frac{d^3\sigma}{dp^3} \right) p_{\ell} dp_{\ell} \theta d\theta \quad (1)$$

(since $p_{\ell} \approx E$ for small θ).

For the muons, we include a decay probability $\lambda_{m_{\pi}}/c\tau_{\pi} \approx \lambda_{m_{\pi}}/c\tau_{\ell}$, i.e.

$$\begin{aligned} \sigma_{\mu} &\approx \int \left(E \frac{d^3\sigma}{dp^3} \right) \frac{dp_{\ell} dp_{\ell}^2}{E} \left(\frac{\lambda_{m_{\pi}}}{c\tau_{\ell}} \right) \\ &\approx 2\pi \int \left(E \frac{d^3\sigma}{dp^3} \right) \left(\frac{\lambda_{m_{\pi}}}{c\tau} \right) dp_{\ell} \theta d\theta . \end{aligned} \quad (2)$$

Here ℓ is the decay length, i.e. a function of θ . For π production, we parametrized the data of Sens et al.⁷⁾ and Capiluppi et al.⁸⁾ as

$$E \frac{d^3\sigma}{dp^3} = A e^{-b p T}$$

at various x from 0.1 to 1.0. For each x , we integrated the cross-section accepted by the spectrometer. This result was then parametrized as

$$\frac{d\sigma}{p_\ell dp_\ell} = A' e^{-b' x},$$

and integrated above p_ℓ^{\min} as in (1) and (2) to obtain the cross-section of Table 2. The decay length is $\ell = \ell_0 + \delta/\theta$, where $\ell_0 = 17$ cm is an absorption length in steel, and δ is the distance of the beam from the wall. Note that by scanning the beam intersection up and down, we vary the $\mu^+\mu^-$ contamination, and can thus extrapolate the "direct muon pairs" directly.

Table 2

Acceptance for $\pi \rightarrow \mu$ produced μ 's,
in angular region $50 < \theta < 110$ mrad

p_μ cut-off (GeV/c)	Beam-wall distance (cm)	σ_π (mb)	σ_{μ^+} (μ b)	μ^+/π ($\times 10^{-4}$)	$\mu^+\mu^-/\pi$ ($\times 10^{-8}$)	$\sigma_{\mu^+\mu^-}$ (mb)
2.6	1	5.3	4.4	8.0	5.9	0.31
	3		8.6	16.0	24.0	1.3
	5		12.8	24.0	53.0	2.9
4.0	1	3.4	2.2	6.4	2.5	0.085
	3		4.4	13.0	10.0	0.34
	5		6.6	19.5	22.0	0.76
5.3	1	2.1	1.1	5.3	1.0	0.020
	3		2.2	11.0	3.9	0.080
	5		3.3	16.7	8.8	0.20

Assuming that cross-section for $\mu^+\mu^-$ from diffractively produced π 's is reduced by a factor ~ 10 , one obtains a "typical" $\mu^+\mu^-$ contamination cross-section for beam centered (3 cm), 4 GeV p_μ cut-off:

$$\sigma_{\mu^+\mu^-} = 0.34 \text{ nb} \times 0.1 = 3.4 \times 10^{-8} \text{ mb.}$$

If one assumes charm production of $1 \mu\text{b}$, $1/4$ probability of $\mu^+\mu^-$ decay scheme, acceptance for μ^+ , μ^- of 0.2 , 0.1 .

$$\sigma_{\mu^+\mu^-}(C) = 10^{-3} \text{ mb} \times \frac{1}{4} \times 0.02 = 5 \times 10^{-6} \text{ mb.} \quad Q = \frac{\sigma_{\mu\mu}(C)}{\sigma_{\mu\mu}(\pi)} = \underline{150}.$$

A P P E N D I X

VECTOR MESON STUDIES WITH R604 SET-UP

It has been suggested that the anomalous muon and electron production observed at NAL is associated with vector mesons, e.g., ρ and ϕ . If the cross-section for vector meson production is also anomalously large at small angles this fact can be readily ascertained with the Double Magnet Spectrometer at I6. The efficiency for detecting ρ^0 via its strong decay mode $\rho^0 \rightarrow \pi^+\pi^-$ is in the range 0.04 to 0.45 for momenta 7 - 15 GeV/c and production angles within 50 mrad of the spectrometer axis. For $\phi \rightarrow K^+K^-$ the detection efficiency is more than a factor of two better than for ρ 's. The mass resolution (FWHM) for ρ and ϕ is ≈ 50 MeV and 5 MeV respectively (5 kG magnetic field and MWPC's with 2 mm wire spacing)

The R604 calorimeter in Arm 2 allows us to explore different possible mechanisms for vector meson production:

- 1) Production in the decay of a large mass ($\gtrsim 10$ GeV) diffractively produced state. The trigger is a single proton of appropriate energy Arm 2
- 2) Production in large transverse momentum reactions. The calorimeter might be used to signal missing energy in the forward cone

REFERENCES

- 1) Cronin et al , Contribution to London conference 1974.
- 2) C. Rubbia, private communication.
- 3) Lederman et al., Contribution to London conference 1974.
- 4) Abramov et al , Contribution to London conference 1974.
- 5) Di Lella et al , Report to the ISRC 1974
- 6) Holder et al , NIM 108, 541 (1973).
- 7) Albrow et al , Negative particle production in the fragmentation region at the CERN ISR (February 1973)
Albrow et al , Positive particle production in the fragmentation region at the CERN ISR (Dezember 1973).
- 8) Charged particle production in p-p inclusive reactions at very high energies (February 1974).

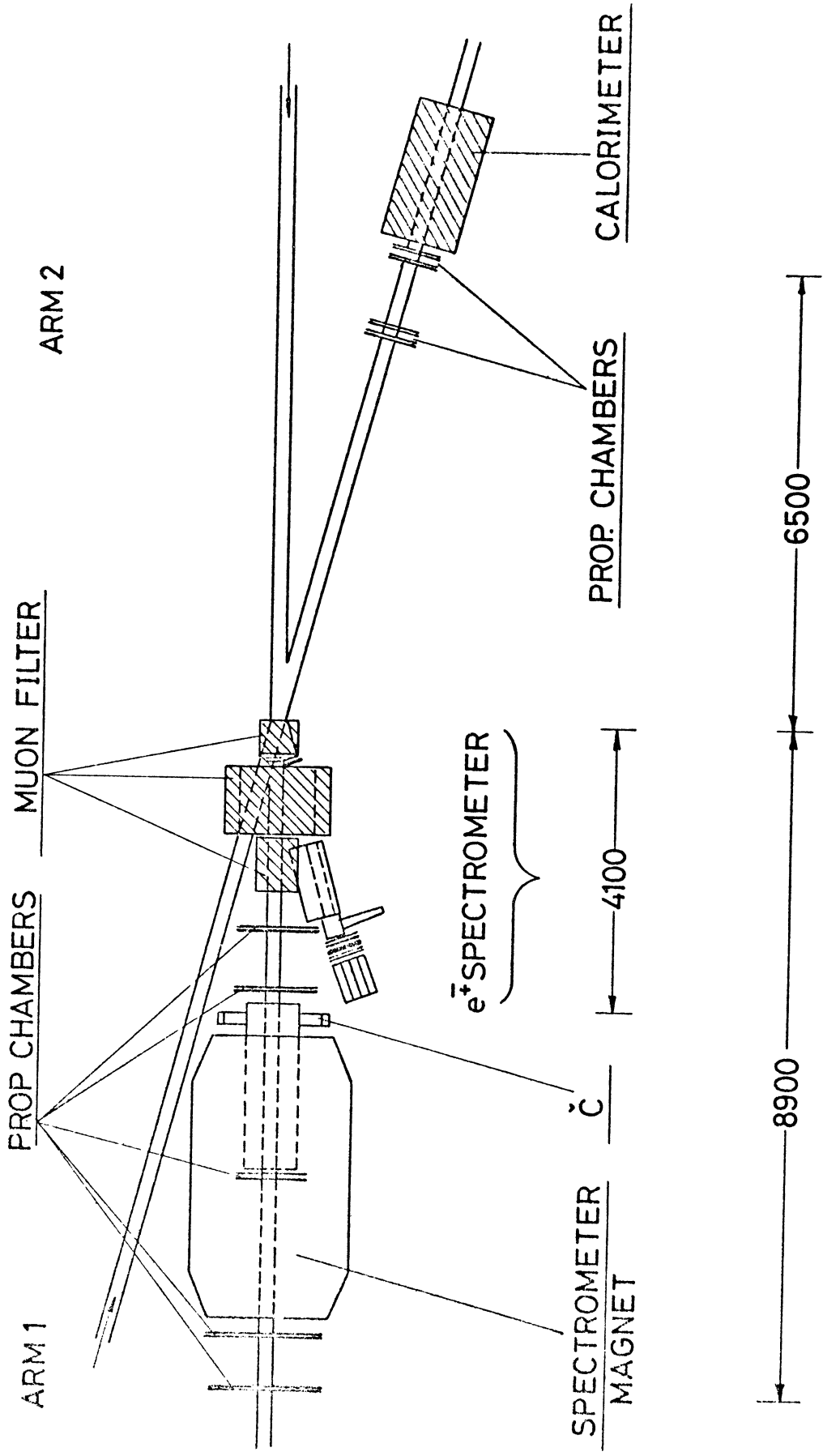


Fig. 1

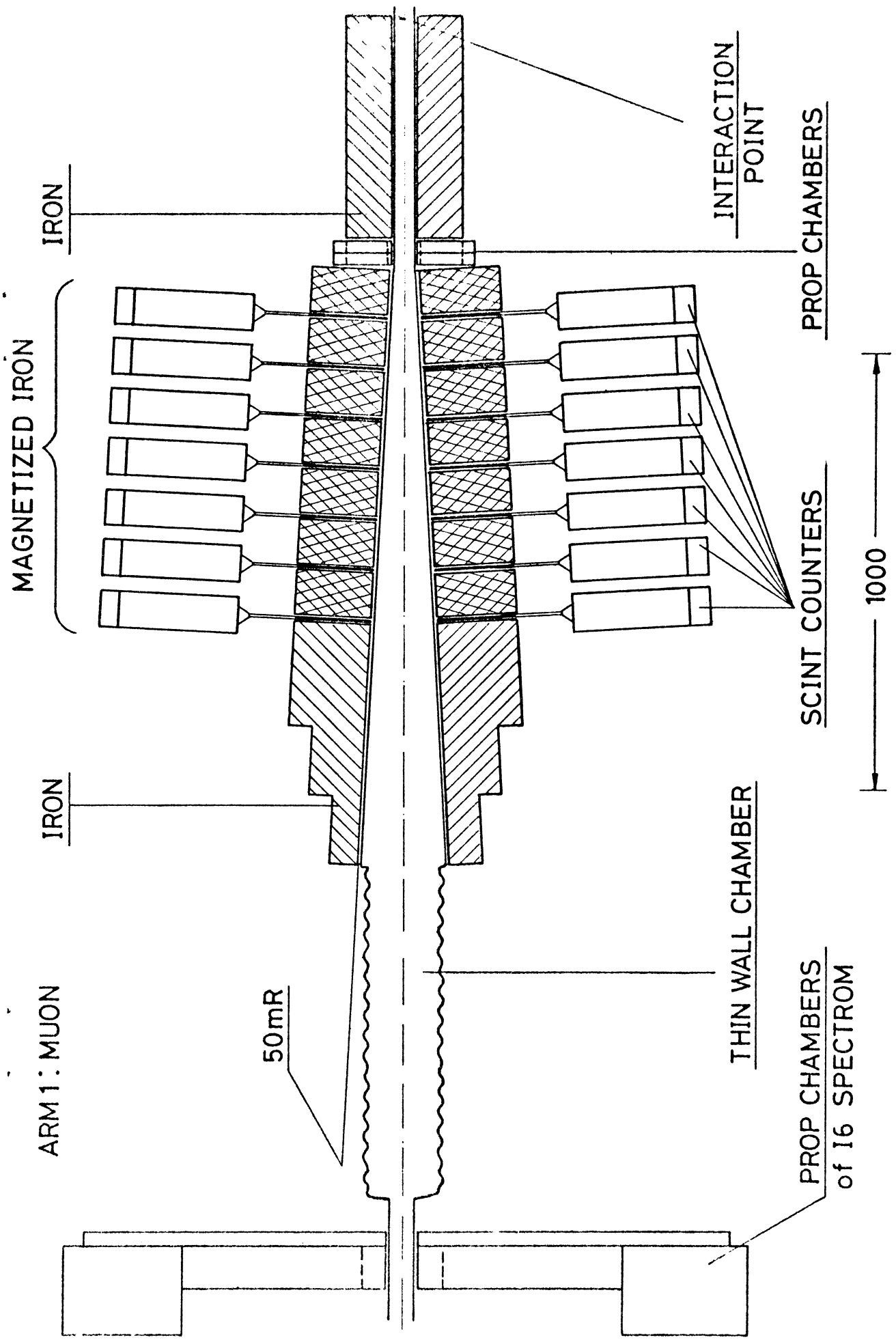


Fig. 2a

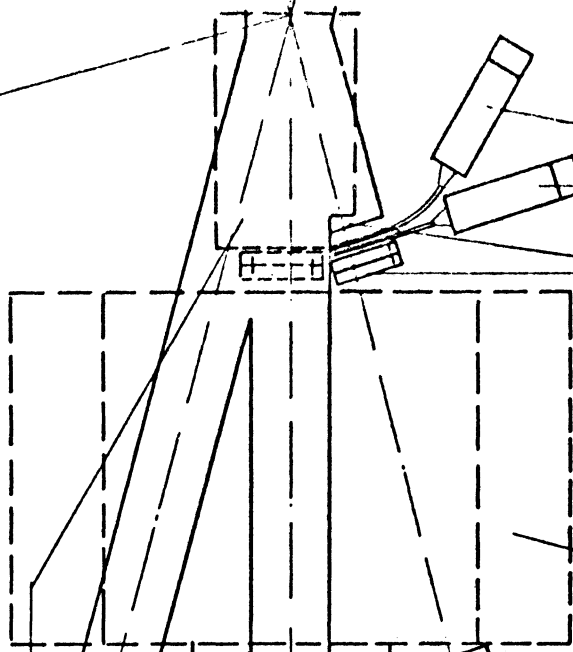
ELEKTRON DETEKTOR

ARM 1

INTERACTION POINT

PROP CHAMBERS
of 16 SPECTROM.

MUON FILTER



THIN WINDOW

MAGNETIZED IRON

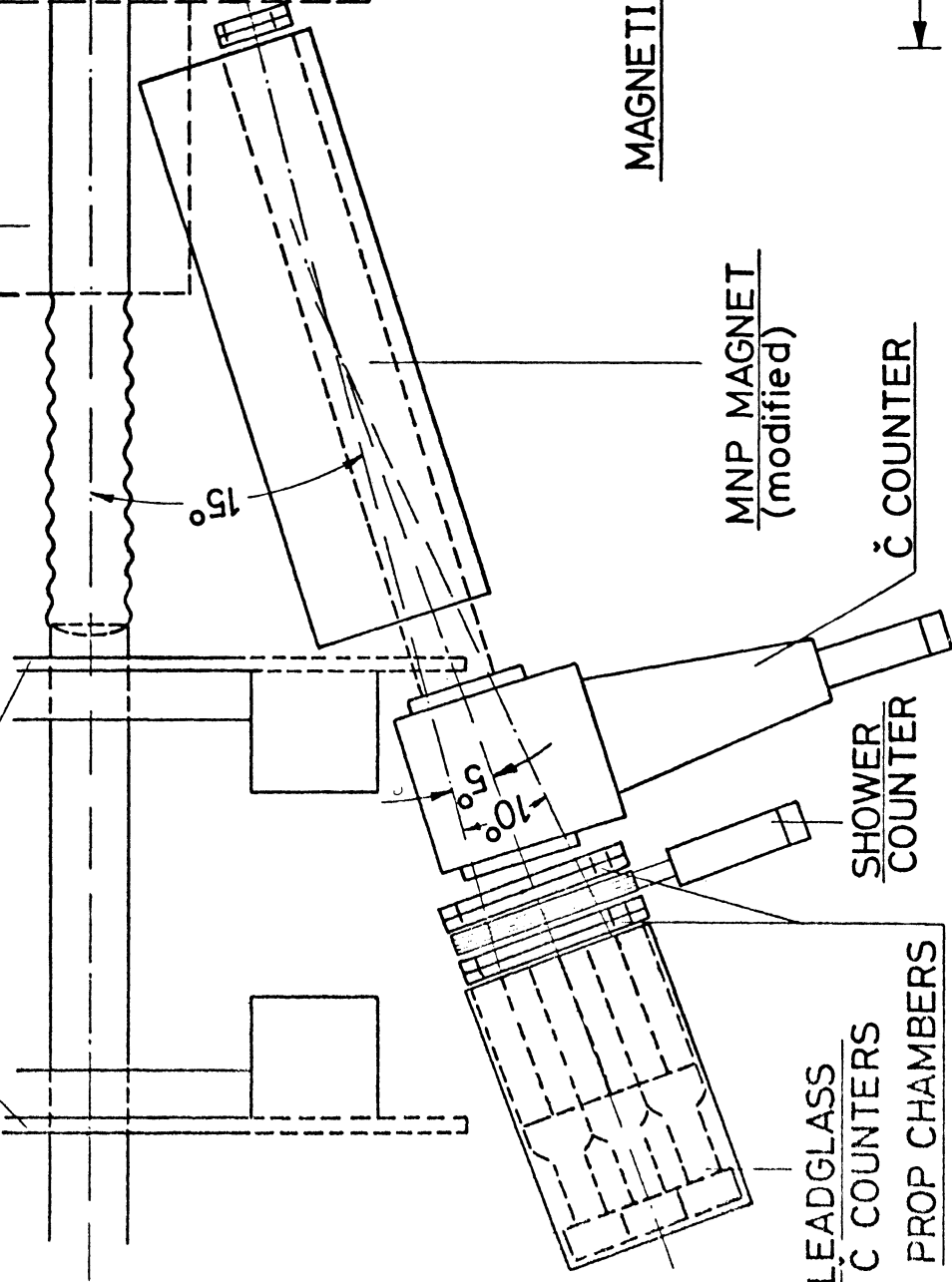
MNP MAGNET
(modified)

PROP CHAMBERS
SCINT COUNT.

Č COUNTER

SHOWER
COUNTER

LEADGLASS
Č COUNTERS
PROP CHAMBERS



1000

Fig. 2b

INTERACTION LENGTH

0.72 1.44 2.16 2.88 3.60 4.30 5.04 5.76 6.48 7.20 7.94 8.66

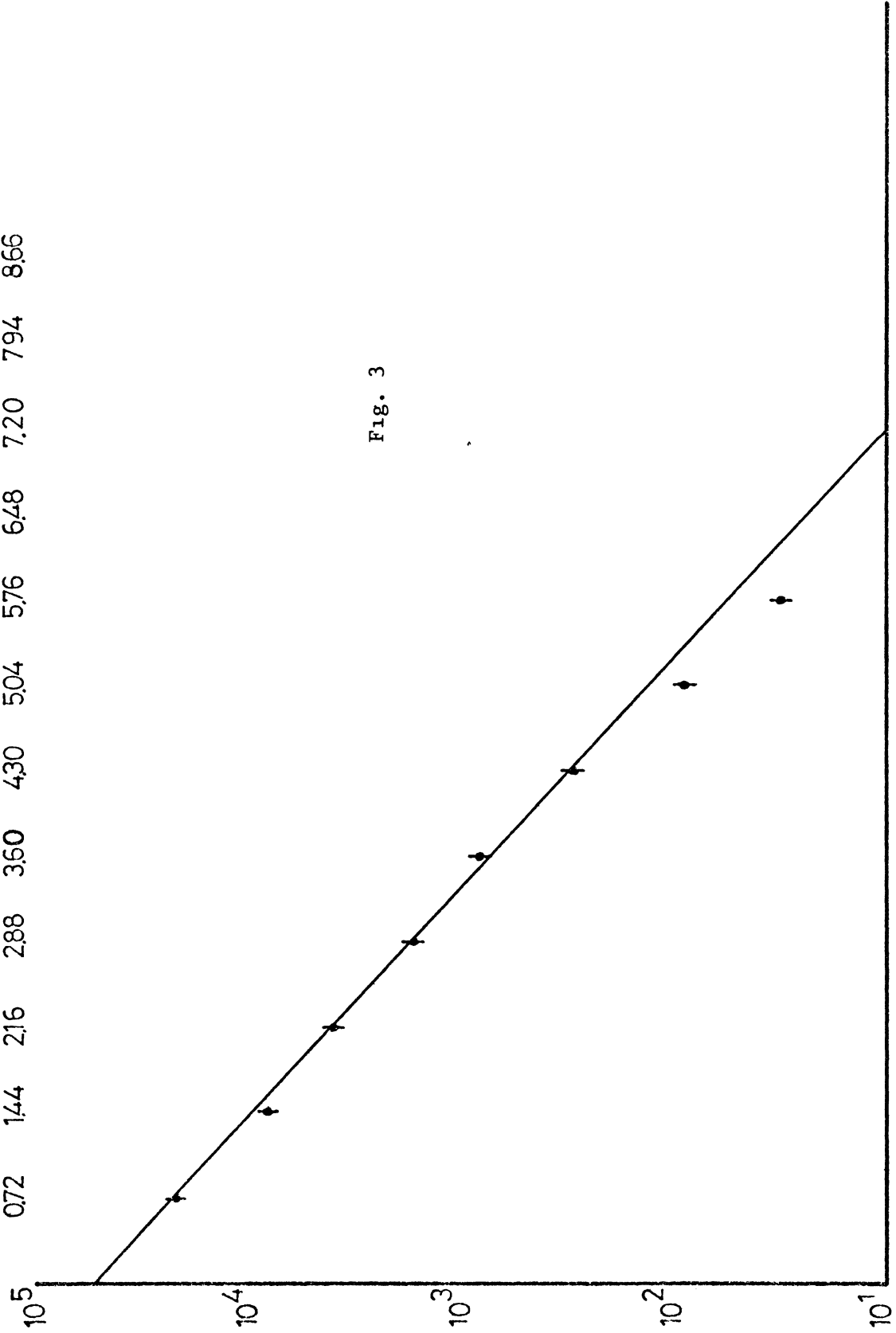
NUMBER OF π^- -WITH NO VISIBLE INTERACTION

10^5
 10^4
 10^3
 10^2
 10^1

1 2 3 4 5 6 7 8 9 10 11 12

NUMBER OF CALORIMETER MODULES TRAVERSED BY π^-

Fig. 3



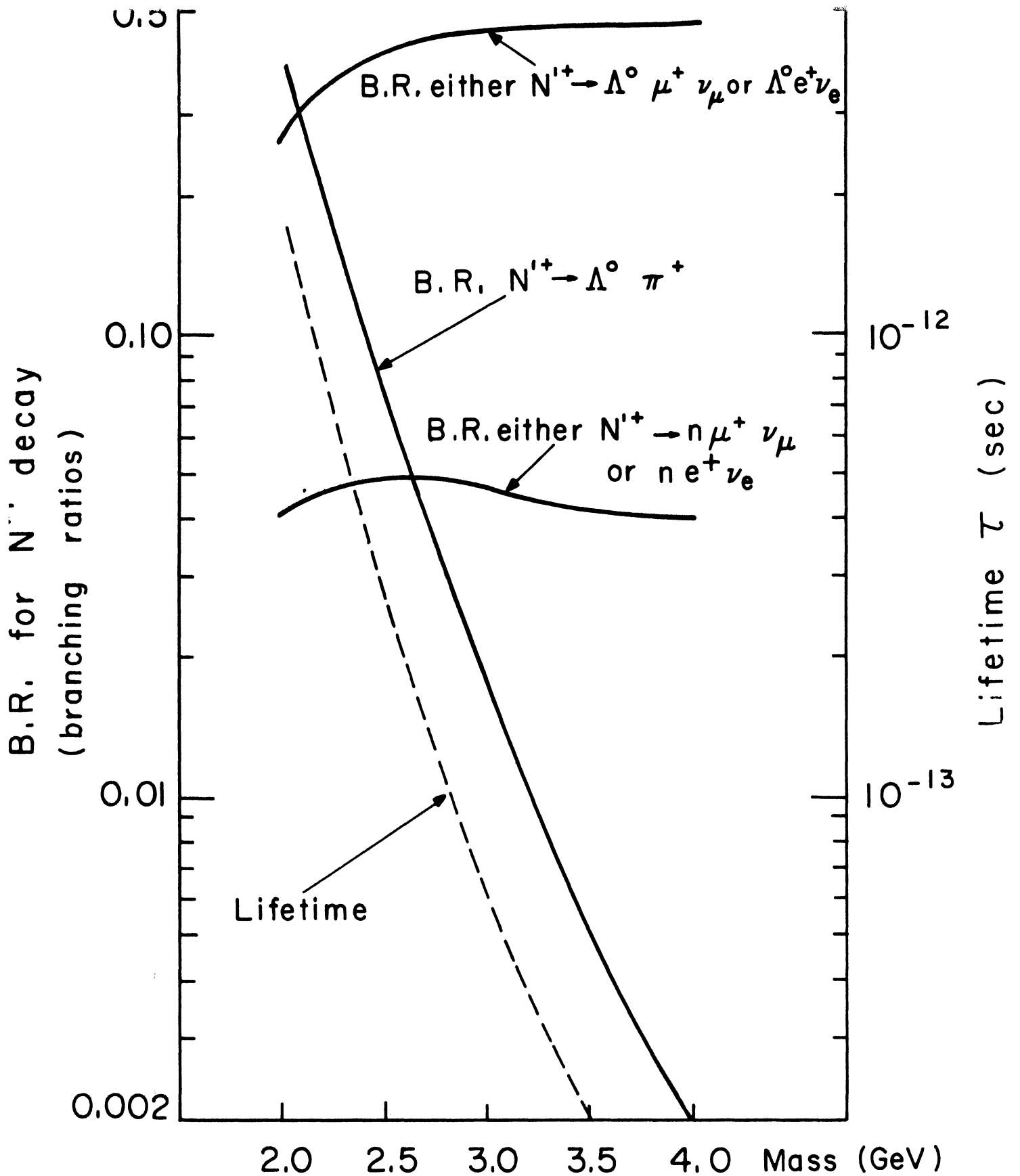


FIG. 4

Lifetime and branching ratios for the singly charmed ($C = +1$) non-strange baryon N'^+ , as a function of its mass, assuming:

- 1) the only decay modes are: $N'^+ \rightarrow \Lambda \ell^+ \nu_\ell$, $N'^+ \rightarrow n \ell^+ \nu_\ell$, $N'^+ \rightarrow \Lambda \pi^+$
- 2) Scaling $\Lambda \rightarrow \pi^- p$ and $\Lambda \rightarrow p e^- \nu_e$ by phase space ratios

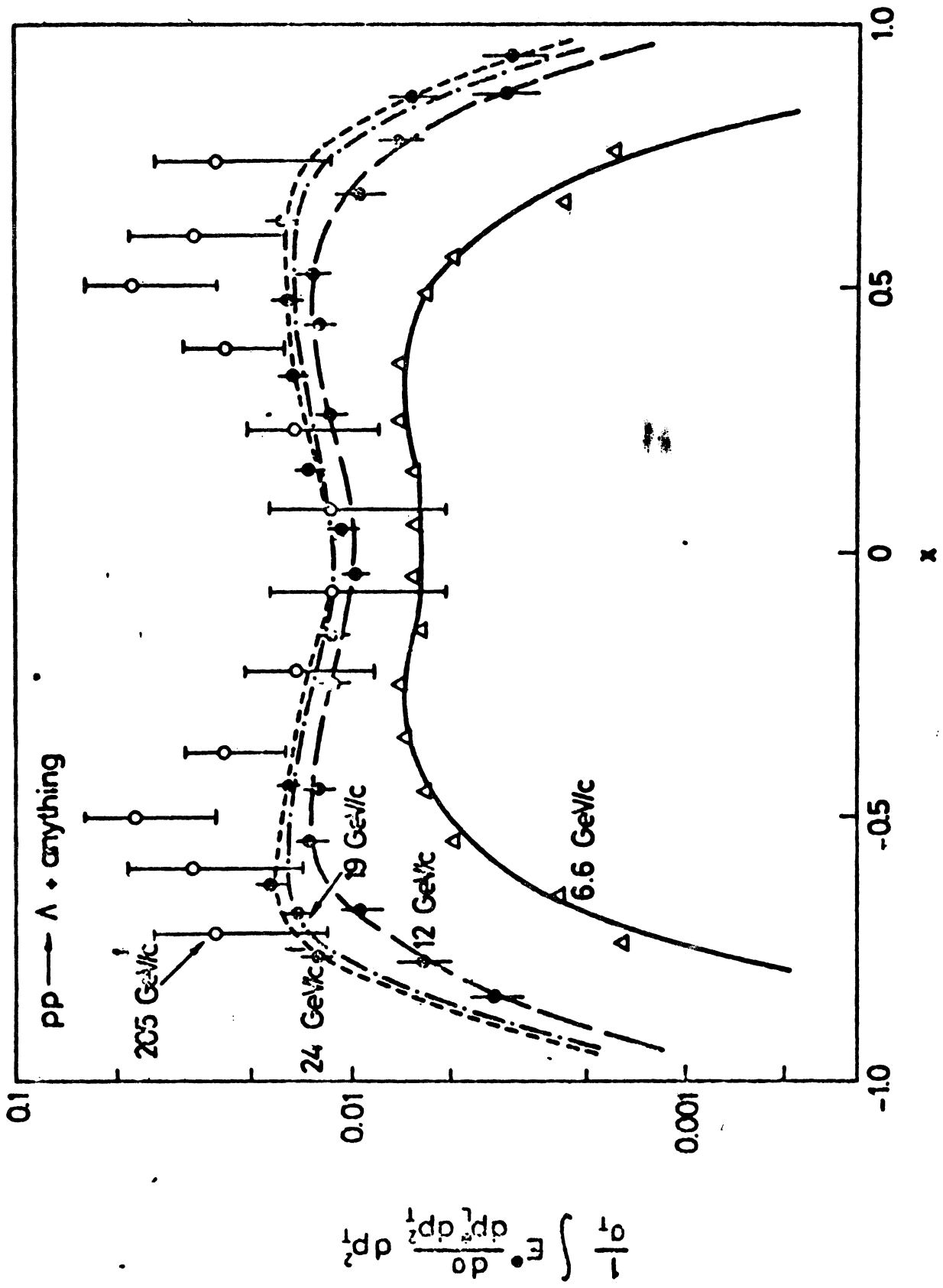


FIG. 5